JACS Au
AN OPEN ACCESS JOURNAL OF THE AMERICAN CHEMICAL SOCIETY

pubs.acs.org/jacsau
Article

Examining the Role of Threonine Phosphorylation in Ubiquitin's Function Using Chemical Protein Synthesis

Bingji Wang,[#] Chuntong Li,[*,#] Fangyu Zhao, Luyu Shi, Xu Li, Yijie Liu, Shuzhe Sun, Ligong Yuan, Maoshen Sun, Yingyue Zhang, Jing Shi,[*] and Lu-Jun Liang[*]

Cite This: JACS Au 2025, 5, 2148−2158

ABSTRACT: The phosphorylation of ubiquitin significantly enhances the complexity of the ubiquitin code. However, the molecular consequences of ubiquitin phosphorylation at threonine residues remain largely uncharacterized. In this study, we present an effective method for the total chemical synthesis of threonine-phosphorylated ubiquitin, producing tens of milligrams of all six in vivo-identified threonine-phosphorylated ubiquitin analogues: pUbT7, pUbT12, pUbT14, pUbT22, pUbT55, and pUbT66. The biochemical activities of phosphorylated ubiquitin analogues were examined in vitro. Our results show that threonine phosphorylation has a differential impact on E2 charging, with phosphorylation at residue Thr7 exhibiting significant inhibition. In addition, threonine phosphorylation significantly affects the E1-E2-E3-mediated assembly and deubiquitinase-mediated disassembly of polyubiquitin chains in a site-specific manner. Collectively, this work provides new insights into the effect of phosphorylation on the ubiquitin code.

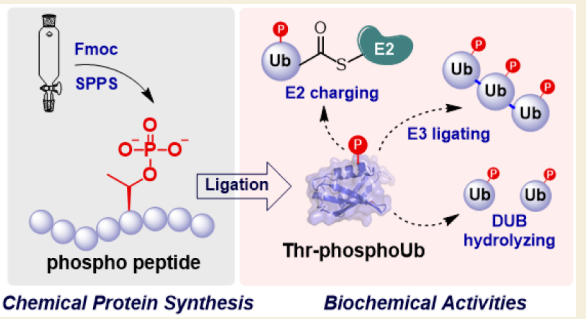

KEYWORDS: *chemical protein synthesis, ubiquitin phosphorylation, threonine phosphorylation, polyubiquitin chain, deubiquitination*

INTRODUCTION

Ubiquitination is a crucial post-translational modification that regulates numerous cellular processes,[1] including protein quality control, the cell cycle, and signal transduction. The ubiquitin modification is orchestrated by a cascade of enzymes,[2] including ubiquitin-activating enzyme (E1), ubiquitin-conjugating enzyme (E2), and ubiquitin ligase (E3). The E1, E2, and E3 act sequentially to attach ubiquitin to the lysine side chain of a substrate. In addition, ubiquitin can be modified on its own seven lysine residues and an N-terminal methionine, resulting in eight distinct types of homogeneous polyubiquitin chains and even more complex heterogeneous polyubiquitin chains.[3−6] Recent studies have revealed that ubiquitin can also be conjugated to serine and threonine residues in proteins, resulting in ester-linked ubiquitin modifications or ubiquitin chains.[7,8] Different ubiquitin chains convey distinct signals. For example, the lysine48 (K48)-linked ubiquitin chain acts as a degradation signal, mediating proteasomal degradation of substrate proteins, while lysine63 (K63)-linked ubiquitin plays an important role in DNA damage repair. Conversely, deubiquitinases (DUBs) hydrolyze the isopeptide bond between ubiquitin and substrate proteins, removing ubiquitin and reversely regulating the ubiquitin modification.[9,10]

Recent studies have revealed that ubiquitin can undergo post-translational modifications,[11−16] including acetylation[11−13] and phosphorylation,[14−16] which, in turn, regulate its structure and function and enhance the complexity of the ubiquitin code. In particular, several sites of phosphorylation have been identified on ubiquitin, including three serine (Ser20, Ser57, and Ser65) residues, six threonine (Thr7, Thr12, Thr14, Thr22, Thr55, and Thr66) residues, and a single tyrosine (Tyr59) residue. Significant progress has been made in understanding the effects of serine and tyrosine phosphorylation on ubiquitin's biochemical activities and structural characteristics (Scheme 1a).[17−23] For example, the kinase PINK1 can specifically phosphorylate ubiquitin at Ser65, resulting in the formation of pUbS65. The pUbS65 alters ubiquitin structure, activates the E3 ligase Parkin,[17] inhibits the polyubiquitination activity of E3 ligases TRAF6 and HOIP,[18] and inhibits the hydrolysis activity of deubiquitinases. Moreover, using a genetic code expansion (GCE) approach, Chin et al. generated serine-phosphorylated ubiquitin (pUbS20, pUbS57, and pUbS65)[21] and found that Ser20 phosphorylation controls the linkage specificity of UBE3C-produced ubiquitin chains. Additionally, Wang et al. developed a GCE approach to generate pUbY59 and found that phosphorylation at Tyr59 altered the conformation of the

Received: January 17, 2025
Revised: March 20, 2025
Accepted: March 21, 2025
Published: April 22, 2025

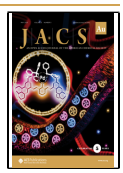

Scheme 1. Investigation of the Effect of Phosphorylation on Ubiquitin. (a) Previous Work, Generation of Serine-Phosphorylated Ubiquitin Using Biological Approaches. (b) This Work, Chemical Synthesis, and Functional Investigations of Threonine-Phosphorylated Ubiquitin

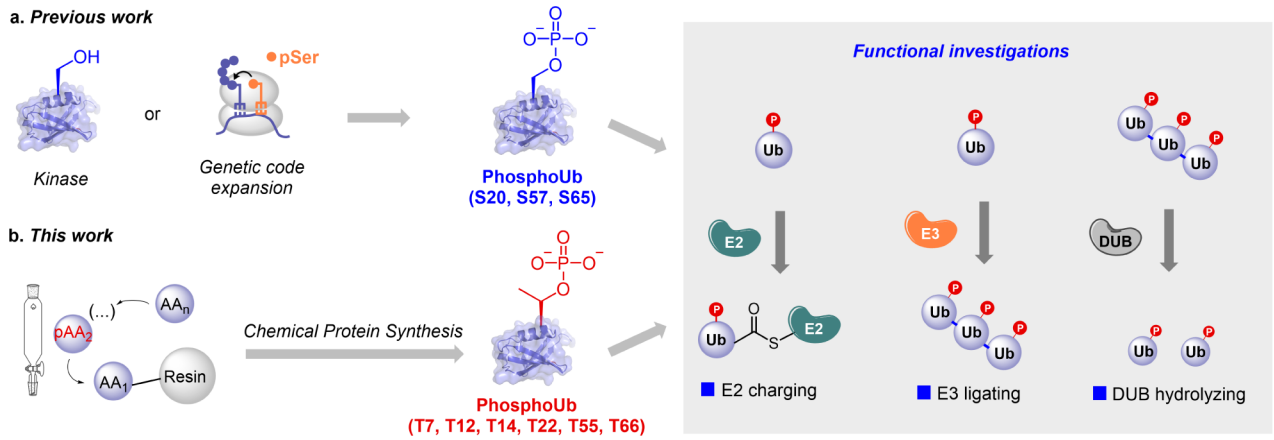

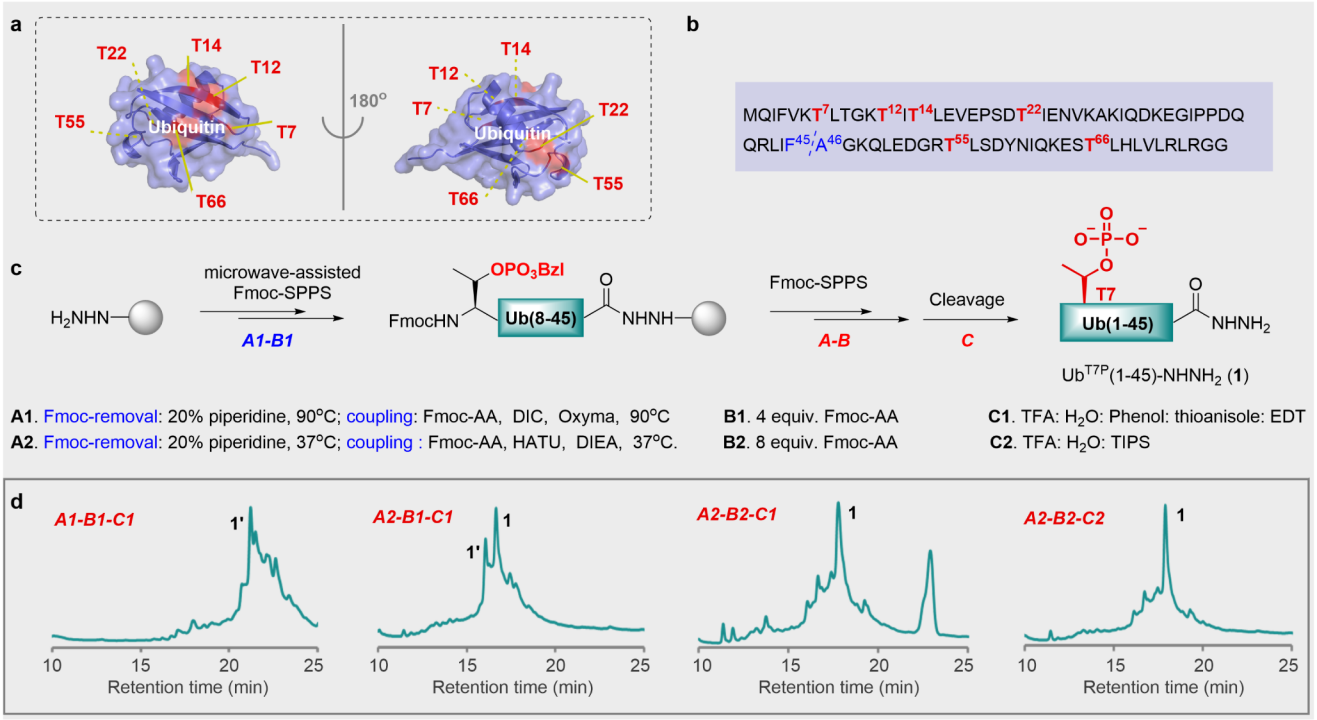

Figure 1. Synthesis of the threonine-phosphorylated ubiquitin segment. (a) Ternary structure of ubiquitin. The phosphorylated threonine sites (T7, T12, T14, T22, T55, T66) were colored in red. (b) The amino-acid sequence of ubiquitin. The phosphorylated threonine sites were colored in red. (c) Optimization of linear solid-phase synthesis of the phosphorylated ubiquitin segment **1**. (d) HPLC analysis of crude peptide obtained after variation of conditions for Fmoc removal and coupling (A1 and A2), the equivalent of Fmoc-AAs (B1 and B2), and TFA cleavage (C1, C2). $Ub^{T7P}(1–45)$-$NHNH_2$ (**1**) and Ub(7–45)-$NHNH_2$ (**1'**).

Y59–E51 loop in ubiquitin and inhibited ubiquitin charging by E2 UBE2D3.[23]

The threonine phosphorylation of ubiquitin was recently shown to play significant physiological roles.[24] Phosphorylation at threonine 12 (pUbT12) functions as a novel histone mark that regulates the DNA damage response by inhibiting the removal of H2AK15Ub by the deubiquitinase USP51. Moreover, pUbT12 prevents the binding of 53BP1 to H2AK15Ub, thereby inhibiting the 53BP1 function at the DNA damage site. Nonetheless, unlike serine and tyrosine residues, which have well-established methods for obtaining site-specifically phosphorylated ubiquitin,[17−23] techniques for accessing homogeneous threonine-phosphorylated ubiquitin remain limited.[25] Consequently, the molecular consequences of ubiquitin threonine phosphorylation remain largely uncharacterized.

Chemical protein synthesis offers a powerful approach to obtain homogeneous proteins with precise post-translational modifications in workable amounts, including phosphorylation, glycosylation, and ubiquitination.[26−29] This approach has been widely applied to functional and structural investigations of numerous proteins with significant biological importance.[30−47] Here, we present an efficient method for the total chemical synthesis of threonine-phosphorylated ubiquitin analogues

https://doi.org/10.1021/jacsau.5c00067
JACS Au 2025, 5, 2148−2158

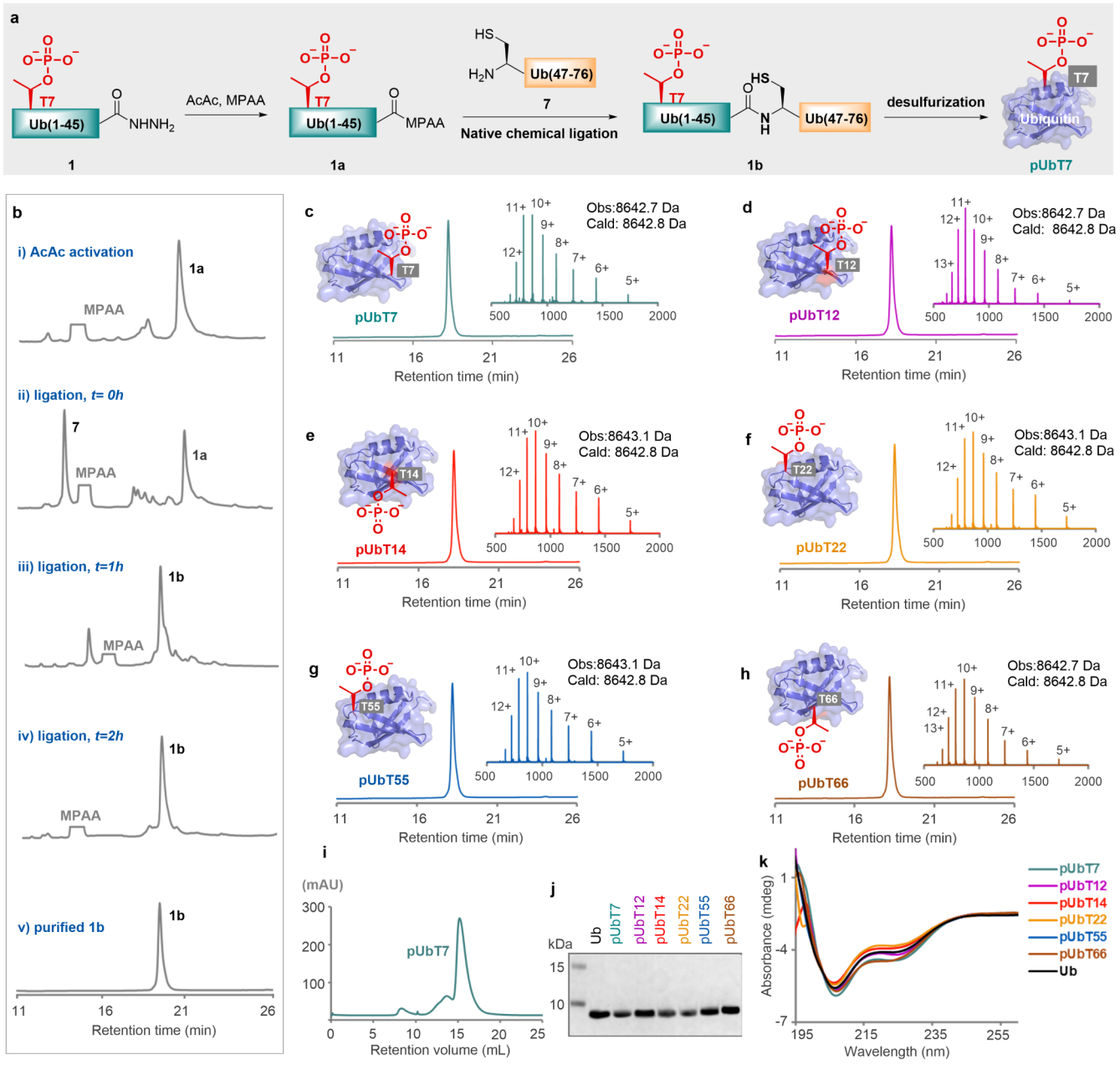

Figure 2. Chemical synthesis and characterizations of threonine-phosphorylated ubiquitin analogues. (a) Synthetic route for Thr7-phosphorylated ubiquitin (pUbT7). (b) Analytical HPLC (214 nm) traces of the native chemical ligation. (c)−(h) Analytical HPLC (214 nm) and ESI-MS of purified phosphorylated ubiquitin analogues (pUbT7, pUbT12, pUbT14, pUbT22, pUbT55, pUbT66). (i) Size exclusion chromatography analysis of the folded pUbT7. (j)−(k) SDS-PAGE analysis and CD spectra of the folded phosphorylated ubiquitin analogues.

(Scheme 1b), including pUbT7, pUbT12, pUbT14, pUbT22, pUbT55, and pUbT66. The synthesized phosphorylated ubiquitin analogues were refolded, and their biochemical activities were examined in vitro. Our experiments show that threonine phosphorylation affects E2 charging, E1-E2-E3-catalyzed assembly, and deubiquitinase-catalyzed disassembly of polyubiquitin chains in a site-specific fashion.

RESULTS AND DISCUSSION

Chemical Synthesis and Characterization of Threonine-Phosphorylated Ubiquitin

The ubiquitin contains 76 amino acid residues, and the identified phosphorylated threonine sites are evenly distributed throughout the sequence of ubiquitin (Figure 1a,b). To improve synthetic efficiency, we designed a synthetic route employing native chemical ligation[48−50] between peptide segments Ub(1−45)-$NHNH_2$ and Ub(46−76) (Figure 1b), followed by postligation desulfurization.[51] Taking the synthesis of phosphorylation at Thr7 (pUbT7) as an example, we initially attempted the single-shot synthesis of the phosphorylated segment Ub^{T7P}(1−45)-$NHNH_2$ (**1**),[49] using microwave-assisted Fmoc-SPPS with 4 equiv of amino acid in coupling reactions, including 4 equivalents of Oxyma and N,N'-diisopropylcarbodiimide (DIC) as a coupling reagent at 90 °C (Figure 1c and Scheme S1, A1−B1−C1). Unfortunately, despite extensive optimization, high-performance liquid chromatography coupled with mass spectrometry (HPLC-

https://doi.org/10.1021/jacsau.5c00067
JACS Au 2025, 5, 2148−2158

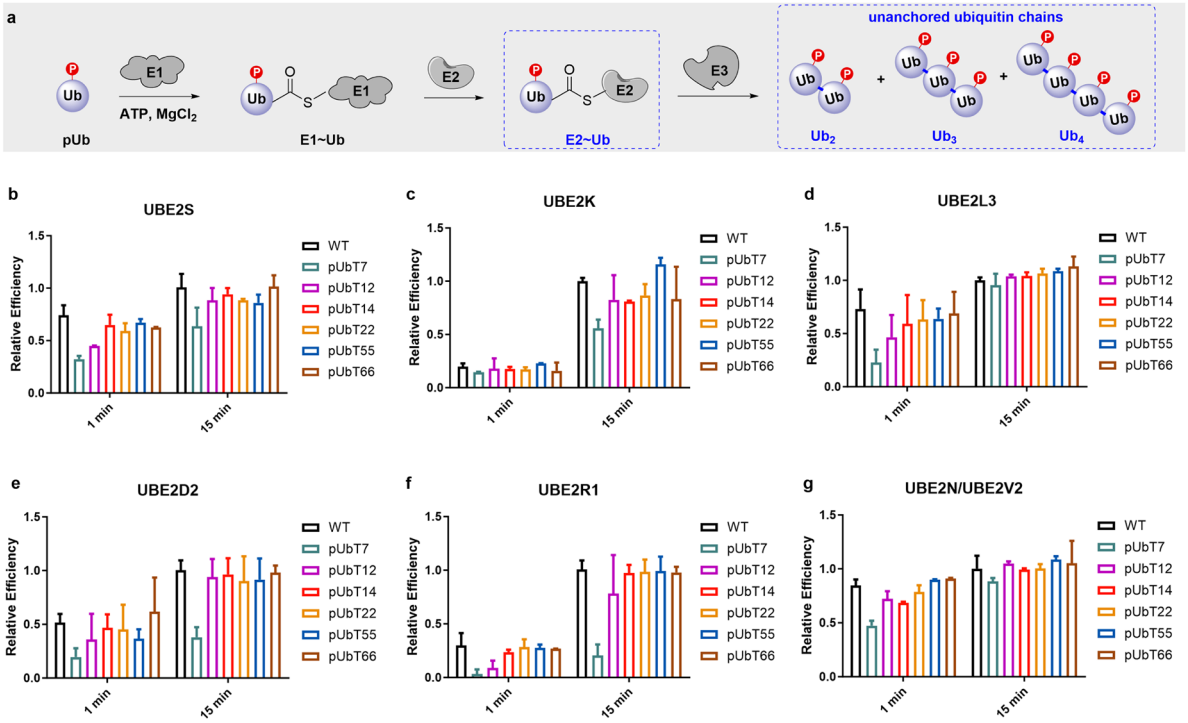

Figure 3. E2 charging is differentially affected by ubiquitin threonine phosphorylation. (a) Schematic representation of E1 activating, E2 charging, and E3 ligating of (phosphorylated) ubiquitin. (b)−(g) Quantitative analysis of the effect of threonine phosphorylation on the efficiencies of Ub charged by six different E2s at 1 and 15 min. Each reaction was performed in two independent biological replicates.

MS) analysis revealed only the byproduct Ub(7−45)-$NHNH_2$ (**1'**) (Figure 1d). To our satisfaction, we first synthesized Fmoc-Ub^{T7P}(7−45) segment using microwave-assisted Fmoc-SPPS at 90 °C (*A1*−*B1*). The remaining sequence after the phosphorylation site was then synthesized at 37 °C using 4 equiv of 2-(7-azabenzotriazol-1-yl)-N,N,N',N'-tetramethyluronium hexafluorophosphate (HATU) and N,N-diisopropylethylamine (DIEA) as a base (*A2*−*B1*) (Figure 1c). HPLC analysis of the crude peptide showed a major peak corresponding to the desired product Ub^{T7P}(1−45)-$NHNH_2$ (**1**), along with a minor peak corresponding to Ub(7−45)-$NHNH_2$ (Figure 1d). Increasing the amount of Fmoc-protected amino acids to 8 equiv for the remaining sequence further improved the synthesis yield (Figure 1d, *A2*−*B2*). Switching the cleavage cocktail TFA/Phenol/H_2O/thioanisole/EDT (*C1*) to TFA/H_2O/TIPS (*C2*) further increased the yield (Figure 1d, *A2*−*B2*−*C2*). Consequently, we optimized a synthetic procedure (*A2*−*B2*−*C2*) for synthesizing the remaining sequence after the threonine phosphorylation site. Starting from 0.2 mmol resin, we were able to synthesize Ub^{T7P}(1−45)-$NHNH_2$ (**1**) within 1 day, isolating over 100 mg of the purified product (Figures S1). Ubiquitin segments phosphorylated at other threonine sites (segments **2**−**6**) were also obtained using the same protocol, yielding over 100 mg each (Figures S2−S6).

With all of the peptide segments in hand, we proceeded to perform native chemical ligation (Figure 2a). Using the synthesis of pUbT7 as an example, Ub^{T7P}(1−45)-$NHNH_2$ (**1**) was dissolved in ligation buffer (100 mM PBS, 6 M Gn-HCl, pH 2.3). Acetylacetone (AcAc, 5 equiv) and 4-mercaptophenylacetic acid (MPAA, 100 equiv) were then added to the reaction to convert segment **1** to the Ub^{T7P}(1−45)-MPAA thioester (**1a**)[47] (Figure 2b). Subsequently, Cys-Ub(47−76)-COOH (**7**, 1.1 equiv) was added to the reaction mixture, and the pH was adjusted to 6.5 to enable native chemical ligation (Figure 2b). The ligation proceeded at room temperature and was completed in 2 h, yielding product **1b** with approximately 60% isolated yield. Following ligation, desulfurization was performed.[51] Briefly, **1b** was dissolved in desulfurization buffer (100 mM PBS, 6 M Gn-HCl, pH 7.4), followed by the addition of VA-044 (30 mM), TCEP (200 mM), and GSH (30 mM). The desulfurization reaction was carried out at 37 °C and completed within 2 h, yielding pUbT7 in 70% isolated yield. In the same way, we obtained pUbT12, pUbT14, pUbT22, pUbT55, and pUbT66 in tens of milligrams (Figures S7−S18), sufficient for biochemical and biophysical investigations. The identity and homogeneity of the phosphorylated ubiquitin analogues were verified by HPLC and ESI-MS analysis (Figure 2c−h). Next, the synthetic phosphorylated ubiquitin analogues were refolded in vitro by gradient dialysis. The refolded proteins were then separated by size-exclusion chromatography, and their purity was confirmed by SDS-PAGE (Figure 2i,j). Circular dichroism (CD) analysis of the phosphorylated ubiquitin analogues revealed absorbance curves similar to those of wild-type ubiquitin (Figure 2k), indicating a correct secondary structure. The phosphorylation sites were confirmed by tryptic-MS/MS analysis (Figures S19−S24).

Phosphorylation at Threonine Sites Differentially Affects E2 Charging

Having synthesized the phosphorylated ubiquitin analogues, we next investigated the impact of threonine phosphorylation on the biochemical activity of ubiquitin (Figure 3a). We first examined the E2 charging step in the ubiquitination process. For the E2 conjugating enzymes, we examined UBE2S and UBE2L3, known for generating free K11-linked ubiquitin chains; UBE2K and UBE2R1, which produce K48-linked

https://doi.org/10.1021/jacsau.5c00067
JACS Au 2025, 5, 2148−2158

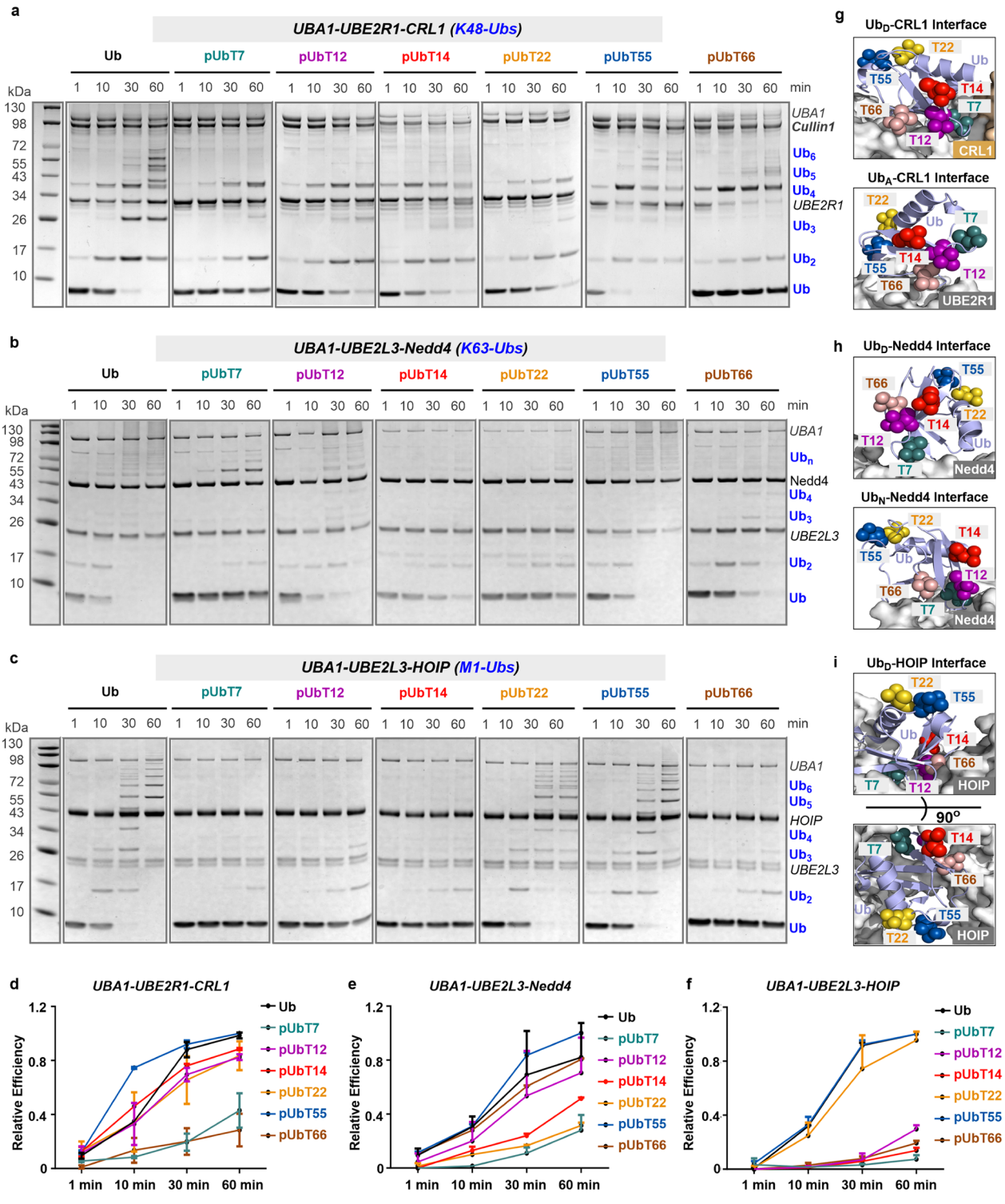

Figure 4. E1-E2-E3-catalyzed assembly of ubiquitin chains is differentially affected by phosphorylation at different threonine residues in ubiquitin. (a–c) Coomassie staining of UBA1-UBE2R1-CRL1-, UBA1-UBE2L3-Nedd4-, and UBA1-UBE2L3-HOIP-catalyzed synthesis of polyubiquitin chains. (d–f) Quantitative analysis of UBA1-UBE2R1-CRL1-, UBA1-UBE2L3-Nedd4-, and UBA1-UBE2L3-HOIP-catalyzed synthesis of polyubiquitin chains. (g) Alignment of predicted structures of phosphorylated ubiquitin analogues with the CRL-UBE2R-catalyzed K48-diUb forging complex (PDB: 8PQL). Top, the donor ubiquitin (Ub_D)-UBE2R1-CRL interaction interface; bottom, the acceptor ubiquitin (Ub_A)-UBE2R1 interaction interface. Ubiquitin is shown as a cartoon, phosphorylated residues are depicted as balls, and the CRL and UBE2R1 are represented as surfaces. (h) Alignment of predicted structures of phosphorylated ubiquitin analogues to the structure of the Nedd4-Ub complex (PDB: 4BBN). Top, the donor ubiquitin (Ub_D)-Nedd4 interaction interface; bottom, the noncovalent ubiquitin (Ub_N)-Nedd4 interaction interface. Ubiquitin is shown as a cartoon, phosphorylated residues are depicted as balls, and Nedd4 are represented as surfaces. (i) Two different views of the alignment of predicted structures of phosphorylated ubiquitin analogues to the structure of HOIP-catalyzed M1-diUb forging complex (PDB: 5EDV). Ubiquitin is shown as a cartoon, phosphorylated residues are depicted as balls, and HOIP are represented as surfaces. Each ubiquitination reaction was performed in two independent biological replicates.

https://doi.org/10.1021/jacsau.5c00067
JACS Au 2025, 5, 2148–2158

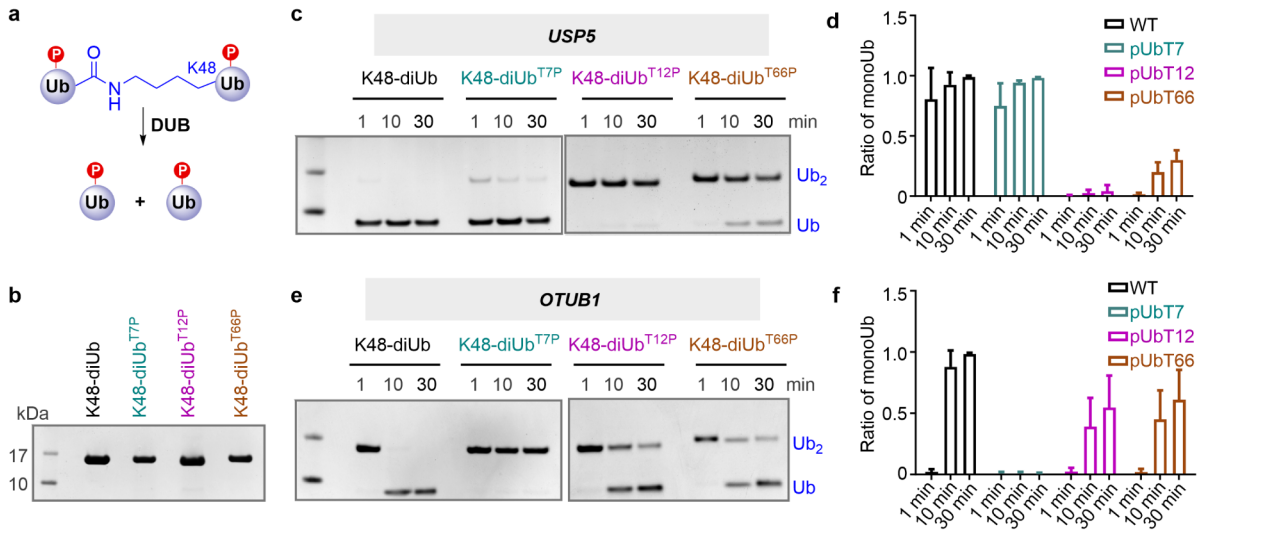

Figure 5. Threonine phosphorylation differentially affects K48-diubiquitin hydrolysis by deubiquitinases. (a) Schematic representation deubiquitinase (DUB) hydrolyzing of (phosphorylated) diubiquitin. (b) SDS-PAGE characterization of purified threonine-phosphorylated K48-linked ubiquitin chains. (c)−(d) Coomassie staining and quantitation of USP5 catalyzed hydrolysis of threonine-phosphorylated K48-linked diubiquitin. Each reaction was performed in two independent biological replicates. (e)−(f) Coomassie staining and quantitation of OTUB1 catalyzed hydrolysis of threonine-phosphorylated K48-linked diubiquitin. Each reaction was performed in two independent biological replicates.

polyubiquitin chains; and UBE2N/UBE2V2, which generates K63-linked polyubiquitin chains.[52] We also examined UBE2D2 that can generate nonspecific ubiquitin chains.[52] To this end, each ubiquitin analogue (10 μM) was incubated with E1 (0.5 μM) and E2 (5 μM) in reaction buffer (50 mM HEPES pH 7.5, 150 mM NaCl, 5 mM ATP, 5 mM $MgCl_2$) at 37 °C. The reactions were analyzed by SDS-PAGE, and we calculated the E2 charging efficiency by (band intensity of E2 ~ Ub)/(band intensity of E2 ~ Ub + band intensity of E2). According to quantified results, compared to wild-type Ub, at a short reaction time frame (1 min), except for UBE2K, the phosphorylation at Thr7 significantly inhibited E2 charging (>50% inhibition), while phosphorylation at other threonine residues had minimal inhibitory effects (10−20% inhibition) (Figures 3b−g and S31). At the 30-min reaction time, the phosphorylation at Thr7 still inhibited ubiquitin charging by UBE2K, UBE2D2, and UBE2R1 (>50% inhibition), while phosphorylation at other threonine residues had minimal inhibitory effect (<20% inhibition) (Figure 3b−g). Based on these observations, we conclude that threonine phosphorylation at different sites in Ub differentially affects its E2-charging activity.

Threonine Phosphorylation Exerts a Site-Specific Influence on E1-E2-E3-Catalyzed Polyubiquitin Chain Assembly

Subsequently, to investigate the impact of threonine phosphorylation on E1-E2-E3-catalyzed polyubiquitin chain assembly (Figure 3a), we examined three types of E3 ligases: (1) the RING (really interesting new gene) family E3 Cullin1-Rbx1 (CRL1), which functions in conjunction with E2 UBE2R1 to produce K48-linked ubiquitin chains;[53] (2) the HECT (homologous to E6AP C-terminus) family E3 NEDD4, which produces K63-linked ubiquitin chains;[54] and (3) the RBR (RING-between-RING) family E3 HOIP, which generates M1-linked linear ubiquitin chains.[55,56] Each phosphorylated ubiquitin (40 μM) was incubated with E1 (0.5 μM), E2 (5 μM), and E3 (2 μM) in reaction buffer (50 mM HEPES pH 7.5, 150 mM NaCl, 5 mM ATP, 5 mM $MgCl_2$) at 37 °C. We analyzed the reaction by SDS-PAGE (Figure 4a−c) and assessed the efficiency of polyubiquitin chain formation by calculating the (band intensity of free Ub chains)/(band intensity of free Ub chains+ band intensity of monoUb) (Figure 4d−f). We found that for the UBA1-UBE2R1-CRL1-catalyzed K48-linked ubiquitin chain formation, phosphorylation at Thr7 and Thr66 significantly inhibited polyubiquitin chain formation (>60% inhibition) across all reaction time frames, phosphorylation at Thr12, Thr14, and Thr22 had a minimal inhibitory effect (20−40% inhibition), while phosphorylation at Thr55 had a slight activation effect at 10 and 30 min (20−30% activation) (Figure 4d). We predicted the structures of phosphorylated ubiquitin analogues using AlphaFold3[57] and aligned them to the reported structures of the CRL-UBE2R-mediated K48-linked ubiquitin chain elongation complex[58] (PDB: 8PQL) (Figure 4g). Thr7 and Thr66 are located at the interface between the donor ubiquitin, Rbx1, and UBE2R1 (Figure 4g). In addition, Thr66 resides at the interface between the acceptor ubiquitin and the acidic loop of UBE2R1 (Figure 4g). Therefore, phosphorylation of Thr7 and Thr66 may lead to electrostatic repulsion and steric clashes. In contrast, Thr55 is solvent-exposed; therefore, phosphorylation might have a minimal impact.

For UBA1-UBE2L3-Nedd4-catalyzed K63-linked ubiquitin chain formation, phosphorylation at Thr7, Thr14, and Thr22 dramatically inhibited (>60% inhibition) polyubiquitin chain assembly across all reaction time frames, while phosphorylation at Thr12 and Thr66 had a minimal effect (10−20% inhibition). Phosphorylation at Thr55 showed a slight activation effect (<10% activation) at 30 and 60 min (Figure 4e). Aligning the predicted structures of phosphorylated ubiquitin analogues to the structure of the Nedd4-Ub complex[59] (PDB: 4BBN) revealed that only Thr7 is located in the Nedd4-Ub_D interface, while the other threonine residues are solvent-exposed (Figure 4h). For the noncovalent Ub-Nedd4 interface, Thr7 and Thr12 are situated in the interface, while the other four sites are solvent-exposed (Figure 4h). Phosphorylation at Thr7 and Thr12 could impair ubiquitin

https://doi.org/10.1021/jacsau.5c00067
JACS Au 2025, 5, 2148−2158

binding, whereas the effects of phosphorylation at the other sites may not be significant. Consequently, the current structure does not provide an explanation for the inhibitory effect of Thr14 and Thr22 phosphorylation; it is possible that phosphorylation may affect the recognition of the acceptor ubiquitin by Nedd4.

For UBA1-UBE2L3-HOIP-catalyzed linear ubiquitin chain formation, phosphorylation at Thr7, Thr12, Thr14, and Thr66 significantly attenuated (>60% inhibition) the generation of linear polyubiquitin chains across all reaction time frames. Phosphorylation at Thr22 had a minimal inhibitory effect (10−20% inhibition), while phosphorylation at Thr55 showed a negligible effect (<5% inhibition) (Figure 4f). Aligning the predicted structures of phosphorylated ubiquitin analogues to the structure of the HOIP-UBE2D2-Ub complex[60] (PDB: 5EDV) showed that residues Thr7, Thr12, Thr14, and Thr66 are located in the HOIP-Ub interface, whereas Thr22 and Thr55 are solvent-exposed (Figure 4i). This structural arrangement could explain the observed effect of threonine phosphorylation on HOIP-catalyzed ubiquitin chain assembly.

Taken together, these findings indicate that threonine phosphorylation exerts a site-specific influence on the E1-E2-E3-catalyzed polyubiquitin chain assembly. For the same threonine site, phosphorylation can have diverse effects on different E1-E2-E3s, and for the same E1-E2-E3 pair, phosphorylation at different threonine sites can elicit distinct impacts.

Threonine Phosphorylation Differentially Affects K48-Linked Ubiquitin Chain Hydrolysis by Deubiquitinases

On the other hand, deubiquitinases (DUBs) reverse ubiquitination by cleaving ubiquitin or ubiquitin chains from substrate proteins.[9,10] We next investigated the influence of ubiquitin threonine phosphorylation on the hydrolytic activity of DUBs toward ubiquitin chains (Figure 5a). The K48-linked ubiquitin chain is one of the most abundant ubiquitin chains in cells, known for acting as a proteasomal degradation signal.[61] To this end, using synthetic phosphorylated ubiquitin monomers as starting material, we employed the K48-specific E2 enzyme UBE2K to generate Thr7-, Thr12-, and Thr66-phosphorylated K48-linked diubiquitins, whose identities were confirmed by SDS-PAGE and tryptic-MS/MS analysis (Figures 5b and S25−S30). We first examined the ubiquitin specific protease (USP) family deubiquitinases USP5 and USP16, which exhibit promiscuous preferences toward eight types of ubiquitin chains.[62] Phosphorylated diubiquitin (5 μM) was incubated with USP5/USP16 (0.25 μM), and the reaction was analyzed by SDS-PAGE at the indicated time points. We assessed the efficiency of deubiquitination by calculating the ratio of (band intensity of monoUb)/(band intensity of monoUb + band intensity of di-Ub). Compared to wild-type K48-linked diubiquitin, which can be completely hydrolyzed by USP5 within 10 min, phosphorylation decreased its hydrolysis by USP5 (Figure 5c,d). Specifically, Thr7 phosphorylation caused slight inhibition (∼10% inhibition at 1 min), Thr66 phosphorylation resulted in substantial inhibition (∼70% inhibition at 30 min), and Thr12 phosphorylation almost completely abolished hydrolysis (>95% inhibition at 30 min). For USP16, we also found that Thr7 phosphorylation had a moderate inhibitory effect (∼50% inhibition at 30 min), while Thr12 and Thr66 phosphorylation completely abolished (>95% inhibition at 30 min) diubiquitin hydrolysis (Figure S32). Finally, we examined the ovarian tumor protease (OTU) family deubiquitinase OTUB1, which exhibits strict specificity toward K48-linked ubiquitin chains. In contrast, we found that Thr7 phosphorylation completely abolished (>95% inhibition at 30 min) K48-diUb hydrolysis, while Thr12 and Thr66 phosphorylation resulted in moderate inhibition (∼50% inhibition at 30 min) (Figure 5e,f). Collectively, the above results suggest that threonine phosphorylation site-specifically affects DUB-catalyzed polyubiquitin chain disassembly.

Deubiquitinases bind to sites in both distal (Ub_D) and proximal ubiquitin (Ub_P) moieties to recognize the ubiquitin chain. Aligning the predicted structures of phosphorylated ubiquitin analogues to the reported structures of USP5-Ub^D (PDB: 3IHP) and USP16-Ub^D (PDB: 8WG5) complexes (Figures S32 and 33),[63] we found that Thr12 and Thr66 are buried at the interfaces between USP5/USP16 and the distal ubiquitin. Therefore, phosphorylation at Thr12 and Thr66 may be incompatible with binding to USP5 and USP16. In contrast, Thr7 is located near the USP5/USP16-Ub interface and is partially solvent-exposed, which could explain the minimal impact of phosphorylation. Additionally, analysis of the structure of the OTUB1-Ub (PDB: 4DDG) complex[64] revealed that Thr7 is located in the interface between OTUB1 and distal ubiquitin, while the residues Thr12 and Thr66 are solvent-exposed (Figure S33). Thus, the current structure of OTUB1 bound to ubiquitin does not provide an explanation for the inhibitory effect of Thr12 and Thr66 phosphorylation on OTUB1-catalyzed K48-linked diubiquitin cleavage. It is possible that phosphorylation may affect the recognition of the proximal ubiquitin by OTUB1.

CONCLUSION

In this study, we reported the expedient total chemical synthesis of workable quantities of threonine-phosphorylated ubiquitin analogues, which were difficult to access through traditional biological approaches. Based on this, we first examined the role of threonine phosphorylation (at Thr7, Thr12, Thr14, Thr22, Thr55, and Thr66) in the ubiquitin conjugation and deconjugation processes. Our experimental results revealed that ubiquitin threonine phosphorylation affected the activities of E2s, E3s, and deubiquitinases in a site-specific manner, providing substantial new insights into the consequences of ubiquitin threonine phosphorylation on its E2, E3, and DUB activity.

Compared to serine phosphorylation, which had a negligible impact on E2 conjugation of ubiquitin, phosphorylation at Thr7 significantly inhibited E2 conjugation of ubiquitin. In contrast, both threonine and serine phosphorylation differentially influenced E3-mediated polyubiquitin chain assembly and DUB-mediated ubiquitin chain disassembly in a site-specific manner (Figure S34). Notably, compared to previous studies, our results suggested that phosphorylation at residues in close proximity can exert distinct effects. For instance, a previous study showed that phosphorylation at Ser65 enhanced cleavage of K48-diUb by OTUB1, USP5, and USP16,[21] while our results revealed that phosphorylation at Thr66 had an inhibitory effect on these DUBs. Taken together, this study showcases the advantage of chemical protein synthesis in obtaining custom-modified proteins and deepens our understanding of the effect of phosphorylation on ubiquitin function.

https://doi.org/10.1021/jacsau.5c00067
JACS Au 2025, 5, 2148−2158

METHODS

Fmoc-Based Peptide Synthesis

The automatic Fmoc-SPPS was conducted on an automated microwave peptide synthesizer (Liberty Blue 2.0, CEM Corp., U.S.A.) as described previously.[44] Typically, peptide synthesis began with resin swelling in DMF for 5 min. Each synthesis cycle included Fmoc deprotection using 20% piperidine (containing 0.1 M Oxyma) and amino acid coupling using protected amino acids (4 equiv), DIC (8 equiv), and Oxyma (4 equiv). After the synthesis was completed, the resin was washed with DCM three times and dried. Typically, 20 mL of cleavage cocktail (TFA: phenol: H_2O: TIS = 82.5:5:5:2.5) was added to the resin, and the reaction mixture was shaken for 2.5 h at 25 °C to cleave the peptides. The resin was filtered, and the combined filtrate was reduced to about 5 mL by nitrogen bubbling. Subsequently, 40 mL of cold ether was added to the filtrate to precipitate the crude peptide. The crude peptide was then washed with 2 × 40 mL of cold ether.

For manual Fmoc-SPPS, both coupling and deprotection were performed at 37 °C. The coupling reactions were performed with 4.0 equiv of Fmoc-amino acids, 4 equiv of HATU, and 8.0 equiv of DIEA in DMF for 30 min. The deprotection reactions were performed with 20% piperidine for 10 min.

Synthesis of Phospho-Ubiquitin with Native Chemical Ligation

Hydrazide-based native chemical ligation was conducted as described previously.[65,66] Briefly, peptide hydrazide (1.5 mM, 1 equiv) was dissolved in 0.5 mL of ligation buffer (6 M Gn-HCl, 0.1 M NaH_2PO_4, pH 2.3). Then, acetylacetone (7.5 mM, 5 equiv) and MPAA (75 mM, 50 equiv) were added to the reaction and was stirred at room temperature for 4 h to convert the peptide hydrazide to the corresponding thioester. Next, 1.1 equiv N-terminal Cys peptide Cys-Ub(47−76)-COOH (dissolved in 0.4 mL of 6 M Gn-HCl, 0.1 M Na_2HPO_4, pH 7.4) was added to the reaction mixture, and the pH was adjusted to 6.5, stirred at room temperature for 2 h for the ligation. Finally, the ligating product was separated by semipreparative HPLC. For protein desulfurization, the phospho-Ub (0.5 mM) was dissolved in 1.0 mL of desulfurization buffer (6 M Gn-HCl, 0.1 M NaH_2PO_4, pH 7.4). Then, VA-044 (40 mM), TCEP (200 mM), and GSH (30 mM) were added to the reaction, the pH was adjusted to 7.0−7.5, and the mixture was stirred at 37 °C for 2 h. The final desulfurized product was separated by semipreparative HPLC (C4 column) using a gradient of 20−60% B over 30 min.

Phospho-Ubiquitin Refolding

Typically, 20 mg of phospho-ubiquitin was dissolved in 10 mL of 8 M urea solution in a dialysis bag and placed in 300 mL of refolding buffer (8 M urea, 50 mM HEPES, pH 8.0). The buffer was then exchanged to HEPES buffer (50 mM HEPES, 50 mM NaCl, pH 8.0) overnight at 4 °C. The refolded phospho-ubiquitin analogues were further purified on an ÄKTA pure chromatography system with a Superdex 75 10/300 GL column.

In Vitro E2 Conjugating Activity of Phospho-Ubiquitin

For the ubiquitin-conjugating assay, 0.5 μM HUBA1, 5 μM E2, and 10 μM phospho-ubiquitin were mixed in a buffer containing 50 mM HEPES, 150 mM NaCl, 10 mM ATP, and 10 mM $MgCl_2$, pH 7.5, at 37 °C. The reaction was stopped by the addition of an equal volume of LDS loading buffer at the indicated time and analyzed by SDS-PAGE.

In Vitro Synthesis of Isomeric Phospho-Ubiquitin Chains by E1-E2-E3

For the ubiquitin chain assembly assay catalyzed by E1-E2-E3, 0.5 μM HUBA1, 5 μM E2, 2 μM E3, and 40 μM phospho-ubiquitin were mixed in a buffer containing 50 mM HEPES, 150 mM NaCl, 10 mM ATP, 10 mM $MgCl_2$, pH 7.5 at 37 °C for 1 h. The reaction was stopped by the addition of an equal volume of LDS loading buffer and analyzed by SDS-PAGE.

In Vitro Hydrolysis of Phosphorylated Diubiquitin by Deubiquitinases

For the deubiquitination assay, 0.25 μM DUBs and 5 μM diubiquitin were mixed in a buffer containing 50 mM HEPES, 150 mM NaCl, pH 7.5, at 37 °C for the indicated times. The reaction was stopped by the addition of an equal volume of LDS loading buffer and analyzed by SDS-PAGE.

ASSOCIATED CONTENT

Supporting Information

The Supporting Information is available free of charge at https://pubs.acs.org/doi/10.1021/jacsau.5c00067.

Routine reagents and instruments, experimental procedures (including protein expression and purification, synthesis and characterization of peptides and proteins, in vitro ubiquitination and deubiquitination assay, protein refolding, and mass spectrometry analysis), some experimental results (PDF)

AUTHOR INFORMATION

Corresponding Authors

Chuntong Li − *Department of Chemistry, Key Lab of Bioorganic Phosphorus Chemistry and Chemical Biology, Tsinghua University, Beijing 100084, China; Beijing Institute of Life Science and Technology, Beijing 102206, China*; Email: lct20@mails.tsinghua.edu.cn

Jing Shi − *Center for BioAnalytical Chemistry, Hefei National Laboratory of Physical Science at Microscale, University of Science and Technology of China, Hefei 230026, China*; orcid.org/0000-0003-0180-4265; Email: shijing@ustc.edu.cn

Lu-Jun Liang − *Center for BioAnalytical Chemistry, Hefei National Laboratory of Physical Science at Microscale, University of Science and Technology of China, Hefei 230026, China; Beijing Institute of Life Science and Technology, Beijing 102206, China*; Email: lujun@ustc.edu.cn

Authors

Bingji Wang − *Center for BioAnalytical Chemistry, Hefei National Laboratory of Physical Science at Microscale, University of Science and Technology of China, Hefei 230026, China*

Fangyu Zhao − *Center for BioAnalytical Chemistry, Hefei National Laboratory of Physical Science at Microscale, University of Science and Technology of China, Hefei 230026, China; Beijing Institute of Life Science and Technology, Beijing 102206, China*

Luyu Shi − *Center for BioAnalytical Chemistry, Hefei National Laboratory of Physical Science at Microscale, University of Science and Technology of China, Hefei 230026, China*

Xu Li − *Center for BioAnalytical Chemistry, Hefei National Laboratory of Physical Science at Microscale, University of Science and Technology of China, Hefei 230026, China*

Yijie Liu − *Center for BioAnalytical Chemistry, Hefei National Laboratory of Physical Science at Microscale, University of Science and Technology of China, Hefei 230026, China*

Shuzhe Sun − *Department of Chemistry, Key Lab of Bioorganic Phosphorus Chemistry and Chemical Biology, Tsinghua University, Beijing 100084, China; Beijing Institute of Life Science and Technology, Beijing 102206, China*

https://doi.org/10.1021/jacsau.5c00067
JACS Au 2025, 5, 2148−2158

Ligong Yuan − *Department of Thoracic Surgery, the First Affiliated Hospital of USTC, Division of Life Sciences and Medicine, University of Science and Technology of China, Hefei 230001, China*

Maoshen Sun − *Department of Cell Biology, Harvard Medical School, Howard Hughes Medical Institute, Boston, Massachusetts 02115-6027, United States;* orcid.org/0000-0002-8602-4817

Yingyue Zhang − *Center for BioAnalytical Chemistry, Hefei National Laboratory of Physical Science at Microscale, University of Science and Technology of China, Hefei 230026, China*

Complete contact information is available at: https://pubs.acs.org/10.1021/jacsau.5c00067

Author Contributions

#B.W. and C.L. contributed equally to this work.

Notes

The authors declare no competing financial interest.

■ ACKNOWLEDGMENTS

This study was supported by the National Natural Science Foundation of China (No. 22407120 and No. 22377117). This work was also supported by the Beijing Life Science Academy (No. 2023100CC0220) and the Key Scientific Research Foundation of the Education Department of Anhui Province (2022AH051266). We acknowledge the protein chemistry facility at the Center for Biomedical Analysis of Tsinghua University for mass spectrometry analysis.

■ REFERENCES

(1) Komander, D.; Rape, M. The ubiquitin code. *Annu. Rev. Biochem.* **2012**, *81*, 203−229.
(2) Swatek, K. N.; Komander, D. Ubiquitin modifications. *Cell Res.* **2016**, *26*, 399−422.
(3) Yau, R.; Rape, M. The increasing complexity of the ubiquitin code. *Nat. Cell Biol.* **2016**, *18*, 579−586.
(4) Varshavsky, A. The ubiquitin system, autophagy, and regulated protein degradation. *Annu. Rev. Biochem.* **2017**, *86*, 123−128.
(5) Yau, R. G.; Doerner, K.; Castellanos, E. R.; Haakonsen, D. L.; Werner, A.; Wang, N.; Yang, X. W.; Martinez-Martin, N.; Matsumoto, M. L.; Dixit, V. M.; Rape, M. Assembly and function of heterotypic ubiquitin chains in cell-cycle and protein quality control. *Cell* **2017**, *171*, 918−933.
(6) Kulathu, Y.; Komander, D. Atypical ubiquitylation—the unexplored world of polyubiquitin beyond Lys48 and Lys63 linkages. *Nat. Rev. Mol. Cell Biol.* **2012**, *13*, 508−523.
(7) Kelsall, I. R.; Zhang, J.; Knebel, A.; Arthur, J. S. C.; Cohen, P. The E3 ligase HOIL-1 catalyses ester bond formation between ubiquitin and components of the Myddosome in mammalian cells. *Proc. Natl. Acad. Sci. U. S. A.* **2019**, *116*, 13293−13298.
(8) McCrory, E. H.; Akimov, V.; Cohen, P.; Blagoev, B. Identification of ester-linked ubiquitylation sites during TLR7 signalling increases the number of inter-ubiquitin linkages from 8 to 12. *Biochem. J.* **2022**, *479*, 2419−2431.
(9) Mevissen, T. E.; Komander, D. Mechanisms of deubiquitinase specificity and regulation, Annu. *Rev. Biochem.* **2017**, *86*, 159−192.
(10) Clague, M. J.; Urbé, S.; Komander, D. Breaking the chains: deubiquitylating enzyme specificity begets function. *Nat. Rev. Mol. Cell Biol.* **2019**, *20*, 338−352.
(11) Ohtake, F.; Saeki, Y.; Sakamoto, K.; Ohtake, K.; Nishikawa, H.; Tsuchiya, H.; Ohta, T.; Tanaka, K.; Kanno, J. Ubiquitin acetylation inhibits polyubiquitin chain elongation. *EMBO Rep.* **2015**, *16*, 192−201.
(12) Lacoursiere, R. E.; O'Donoghue, P.; Shaw, G. S. Programmed ubiquitin acetylation using genetic code expansion reveals altered ubiquitination patterns. *FEBS Lett.* **2020**, *594*, 1226−1234.
(13) Lacoursiere, R. E.; Shaw, G. S. Acetylated Ubiquitin Modulates the Catalytic Activity of the E1 Enzyme Uba1. *Biochemistry* **2021**, *60* (16), 1276−1285.
(14) Song, L.; Luo, Z.-Q. Post-translational regulation of ubiquitin signaling. *J. Cell Biol.* **2019**, *218*, 1776−1786.
(15) Lacoursiere, R. E.; Hadi, D.; Shaw, G. S. Acetylation, phosphorylation, ubiquitination (oh my!): Following post-translational modifications on the ubiquitin road. *Biomolecules* **2022**, *12*, 467.
(16) Hepowit, N. L.; Kolbe, C. C.; Zelle, S. R.; Latz, E.; MacGurn, J. A. Regulation of ubiquitin and ubiquitin-like modifiers by phosphorylation. *FEBS J.* **2022**, *289*, 4797−4810.
(17) Koyano, F.; Okatsu, K.; Kosako, H.; Tamura, Y.; Go, E.; Kimura, M.; Kimura, Y.; Tsuchiya, H.; Yoshihara, H.; Hirokawa, T.; Endo, T.; Fon, E. A.; Trempe, J.-F.; Saeki, Y.; Tanaka, K.; Matsuda, N. Ubiquitin is phosphorylated by PINK1 to activate parkin. *Nature* **2014**, *510*, 162−166.
(18) Wauer, T.; Swatek, K. N.; Wagstaff, J. L.; Gladkova, C.; Pruneda, J. N.; Michel, M. A.; Gersch, M.; Johnson, C. M.; Freund, S. M.; Komander, D. Ubiquitin Ser65 phosphorylation affects ubiquitin structure, chain assembly and hydrolysis. *EMBO J.* **2015**, *34*, 307−325.
(19) Swaney, D. L.; Rodríguez-Mias, R. A.; Villén, J. Phosphorylation of ubiquitin at Ser65 affects its polymerization, targets, and proteome-wide turnover. *EMBO Rep.* **2015**, *16*, 1131−1144.
(20) Rogerson, D. T.; Sachdeva, A.; Wang, K.; Haq, T.; Kazlauskaite, A.; Hancock, S. M.; Huguenin-Dezot, N.; Muqit, M. M.; Fry, A. M.; Bayliss, R.; Chin, J. W. Efficient genetic encoding of phosphoserine and its nonhydrolyzable analog. *Nat. Chem. Biol.* **2015**, *11*, 496−503.
(21) Huguenin-Dezot, N.; De Cesare, V.; Peltier, J.; Knebel, A.; Kristaryianto, Y. A.; Rogerson, D. T.; Kulathu, Y.; Trost, M.; Chin, J. W. Synthesis of isomeric phosphoubiquitin chains reveals that phosphorylation controls deubiquitinase activity and specificity. *Cell Rep.* **2016**, *16*, 1180−1193.
(22) George, S.; Wang, S. M.; Bi, Y.; Treidlinger, M.; Barber, K. R.; Shaw, G. S.; O'Donoghue, P. Ubiquitin phosphorylated at Ser57 hyper-activates parkin. *Biochim. Biophy. Acta Gen. Subj.* **2017**, *1861*, 3038−3046.
(23) Hoppmann, C.; Wong, A.; Yang, B.; Li, S.; Hunter, T.; Shokat, K. M.; Wang, L. Site-specific incorporation of phosphotyrosine using an expanded genetic code. *Nat. Chem. Biol.* **2017**, *13*, 842−844.
(24) Walser, F.; Mulder, M. P.; Bragantini, B.; Burger, S.; Gubser, T.; Gatti, M.; Botuyan, M. V.; Villa, A.; Altmeyer, M.; Neri, D.; Ovaa, H.; Mer, G.; Penengo, L. Ubiquitin phosphorylation at Thr12 modulates the DNA damage response. *Mol. Cell* **2020**, *80*, 423−436.
(25) Zhang, M. S.; Brunner, S. F.; Huguenin-Dezot, N.; Liang, A. D.; Schmied, W. H.; Rogerson, D. T.; Chin, J. W. Biosynthesis and genetic encoding of phosphothreonine through parallel selection and deep sequencing. *Nat. Methods* **2017**, *14*, 729−736.
(26) Bondalapati, S.; Jbara, M.; Brik, A. Expanding the chemical toolbox for the synthesis of large and uniquely modified proteins. *Nat. Chem.* **2016**, *8*, 407−418.
(27) Sun, Z.; Liu, H.; Li, X. Precision in protein chemical modification and total synthesis. *Chem* **2024**, *10*, 767−799.
(28) Ai, H.; Pan, M.; Liu, L. Chemical synthesis of human proteoforms and application in biomedicine. *ACS Cent. Sci.* **2024**, *10*, 1442−1459.
(29) Dong, S.; Zheng, J.-S.; Li, Y.; Wang, H.; Chen, G.; Chen, Y.; Fang, G.; Guo, J.; He, C.; Hu, H.; Li, X.; Li, Y.; Li, Z.; Pan, M.; Tang, S.; Tian, C.; Wang, P.; Wu, B.; Wu, C.; Zhao, J.; Liu, L. Recent advances in chemical protein synthesis: method developments and biological applications. *Sci. China Chem.* **2024**, *67*, 1060−1096.
(30) Chu, G.-C.; Liang, L.-J.; Zhao, R.; Guo, Y.-Y.; Li, C.-T.; Zuo, C.; Ai, H.; Hua, X.; Li, Z.-C.; Li, Y.-M.; Liu, L. Ferricyanide-Promoted Oxidative Activation and Ligation of Protein Thioacids in Neutral Aqueous Media. *CCS Chem.* **2024**, *6*, 2031−2043.

(31) Msallam, M.; Sun, H.; Meledin, R.; Franz, P.; Brik, A. Examining the role of phosphorylation of p19INK4d in its stability and ubiquitination using chemical protein synthesis. *Chem. Sci.* **2020**, *11*, 5526−5531.
(32) Li, Y.; Heng, J.; Sun, D.; Zhang, B.; Zhang, X.; Zheng, Y.; Shi, W.-W.; Wang, T.-Y.; Li, J.-Y.; Sun, X.; Liu, X.; Zheng, J.-S.; Kobilka, B.; Liu, L. Chemical synthesis of a full-length G-protein-coupled receptor β2-adrenergic receptor with defined modification patterns at the C-terminus. *J. Am. Chem. Soc.* **2021**, *143*, 17566−17576.
(33) Ai, H.; Chu, G.-C.; Gong, Q.; Tong, Z.-B.; Deng, Z.; Liu, X.; Yang, F.; Xu, Z.; Li, J.-B.; Tian, C.; Liu, L. Chemical synthesis of post-translationally modified H2AX reveals redundancy in interplay between histone phosphorylation, ubiquitination, and methylation on the binding of 53BP1 with nucleosomes. *J. Am. Chem. Soc.* **2022**, *144*, 18329−18337.
(34) Piemontese, E.; Herfort, A.; Perevedentseva, Y.; Möller, H. M.; Seitz, O. Multiphosphorylation-Dependent Recognition of Anti-pS2 Antibodies against RNA Polymerase II C-Terminal Domain Revealed by Chemical Synthesis. *J. Am. Chem. Soc.* **2024**, *146*, 12074−12086.
(35) Wang, P.; Dong, S.; Shieh, J.-H.; Peguero, E.; Hendrickson, R.; Moore, M. A.; Danishefsky, S. J. Erythropoietin derived by chemical synthesis. *Science* **2013**, *342*, 1357−1360.
(36) Galashov, A.; Kazakova, E.; Stieger, C. E.; Hackenberger, C. P.; Seitz, O. Rapid building block-economic synthesis of long, multi-O-GalNAcylated MUC5AC tandem repeat peptides. *Chem. Sci.* **2024**, *15*, 1297−1305.
(37) Balana, A. T.; Mahul-Mellier, A.-L.; Nguyen, B. A.; Horvath, M.; Javed, A.; Hard, E. R.; Jasiqi, Y.; Singh, P.; Afrin, S.; Pedretti, R.; et al. O-GlcNAc forces an α-synuclein amyloid strain with notably diminished seeding and pathology. *Nat. Chem. Biol.* **2024**, *20*, 646−655.
(38) Tang, S.; Liang, L. J.; Si, Y. Y.; Gao, S.; Wang, J. X.; Liang, J.; Mei, Z.; Zheng, J. S.; Liu, L. Practical chemical synthesis of atypical ubiquitin chains by using an isopeptide-linked Ub isomer. *Angew. Chem., Int. Ed.* **2017**, *56*, 13333−13337.
(39) Liang, L. J.; Chu, G. C.; Qu, Q.; Zuo, C.; Mao, J.; Zheng, Q.; Chen, J.; Meng, X.; Jing, Y.; Deng, H.; Li, Y.-M.; Liu, L. Chemical synthesis of activity-based E2-ubiquitin probes for the structural analysis of E3 ligase-catalyzed transthiolation. *Angew. Chem., Int. Ed.* **2021**, *60*, 17171−17177.
(40) Wang, T.; Li, C.; Wang, M.; Zhang, J.; Zheng, Q.; Liang, L.; Chu, G.; Tian, X.; Deng, H.; He, W.; et al. Expedient Synthesis of Ubiquitin-like Protein ISG15 Tools through Chemo-Enzymatic Ligation Catalyzed by a Viral Protease Lbpro. *Angew. Chem. Int. Ed. Engl.* **2022**, *61*, No. e202206205.
(41) Tolmachova, K. A.; Farnung, J.; Liang, J. R.; Corn, J. E.; Bode, J. W. Facile preparation of UFMylation activity-based probes by chemoselective installation of electrophiles at the C-terminus of recombinant UFM1. *ACS Cent. Sci.* **2022**, *8*, 756−762.
(42) Kriegesmann, J.; Brik, A. Synthesis of ubiquitinated proteins for biochemical and functional analysis. *Chem. Sci.* **2023**, *14*, 10025−10040.
(43) Li, C.; Wang, T.; Liang, L.; Chu, G.; Zhang, J.; He, W.; Liu, L.; Li, J. Simultaneous capture of ISG15 conjugating and deconjugating enzymes using a semi-synthetic ISG15-Dha probe. *Sci. China Chem.* **2023**, *66*, 837−844.
(44) Liang, L.-J.; Wang, Y.; Hua, X.; Yuan, R.; Xia, Q.; Wang, R.; Li, C.; Chu, G.-C.; Liu, L.; Li, Y.-M. Cell-Permeable Stimuli-Responsive Ubiquitin Probe for Time-Resolved Monitoring of Substrate Ubiquitination in Live Cells. *JACS Au* **2023**, *3*, 2873−2882.
(45) Mikami, T.; Majima, S.; Song, H.; Bode, J. W. Biocompatible lysine protecting groups for the chemoenzymatic synthesis of K48/K63 heterotypic and branched ubiquitin chains. *ACS Cent. Sci.* **2023**, *9*, 1633−1641.
(46) Farnung, J.; Tolmachova, K. A.; Bode, J. W. Installation of electrophiles onto the C-terminus of recombinant ubiquitin and ubiquitin-like proteins. *Chem. Sci.* **2022**, *14*, 121−129.
(47) Shkolnik, D.; Dey, S.; Hasan, M.; Matunis, M. J.; Brik, A. Chemical protein synthesis combined with protein cell delivery reveals new insights on the maturation process of SUMO2. *Chem. Sci.* **2024**, *16*, 191−198.
(48) Dawson, P. E.; Muir, T. W.; Clark-Lewis, I.; Kent, S. B. Synthesis of proteins by native chemical ligation. *Science* **1994**, *266*, 776−779.
(49) Fang, G. M.; Li, Y. M.; Shen, F.; Huang, Y. C.; Li, J. B.; Lin, Y.; Cui, H. K.; Liu, L. Protein chemical synthesis by ligation of peptide hydrazides. *Angew. Chem., Int. Ed.* **2011**, *50*, 7645−7649.
(50) Flood, D. T.; Hintzen, J. C.; Bird, M. J.; Cistrone, P. A.; Chen, J. S.; Dawson, P. E. Leveraging the Knorr pyrazole synthesis for the facile generation of thioester surrogates for use in native chemical ligation. *Angew. Chem., Int. Ed.* **2018**, *57*, 11634−11639.
(51) Wan, Q.; Danishefsky, S. J. Free-radical-based, specific desulfurization of cysteine: a powerful advance in the synthesis of polypeptides and glycopolypeptides. *Angew. Chem., Int. Ed.* **2007**, *46*, 9248−9252.
(52) David, Y.; Ziv, T.; Admon, A.; Navon, A. The E2 ubiquitin-conjugating enzymes direct polyubiquitination to preferred lysines. *J. Biol. Chem.* **2010**, *285*, 8595−8604.
(53) Petroski, M. D.; Deshaies, R. J. Mechanism of lysine 48-linked ubiquitin-chain synthesis by the cullin-RING ubiquitin-ligase complex SCF-Cdc34. *Cell* **2005**, *123*, 1107−1120.
(54) Maspero, E.; Mari, S.; Valentini, E.; Musacchio, A.; Fish, A.; Pasqualato, S.; Polo, S. Structure of the HECT: ubiquitin complex and its role in ubiquitin chain elongation. *EMBO Rep.* **2011**, *12*, 342−349.
(55) Kirisako, T.; Kamei, K.; Murata, S.; Kato, M.; Fukumoto, H.; Kanie, M.; Sano, S.; Tokunaga, F.; Tanaka, K.; Iwai, K. A ubiquitin ligase complex assembles linear polyubiquitin chains. *EMBO J.* **2006**, *25*, 4877−4887.
(56) Stieglitz, B.; Rana, R. R.; Koliopoulos, M. G.; Morris-Davies, A. C.; Schaeffer, V.; Christodoulou, E.; Howell, S.; Brown, N. R.; Dikic, I.; Rittinger, K. Structural basis for ligase-specific conjugation of linear ubiquitin chains by HOIP. *Nature* **2013**, *503*, 422−426.
(57) Abramson, J.; Adler, J.; Dunger, J.; Evans, R.; Green, T.; Pritzel, A.; Ronneberger, O.; Willmore, L.; Ballard, A. J.; Bambrick, J.; et al. Accurate structure prediction of biomolecular interactions with AlphaFold 3. *Nature* **2024**, *630*, 493−500.
(58) Liwocha, J.; Li, J.; Purser, N.; Rattanasopa, C.; Maiwald, S.; Krist, D. T.; Scott, D. C.; Steigenberger, B.; Prabu, J. R.; Schulman, B. A. Mechanism of millisecond Lys48-linked poly-ubiquitin chain formation by cullin-RING ligases. *Nat. Struct. Mol. Biol.* **2024**, *31*, 378−389.
(59) Maspero, E.; Valentini, E.; Mari, S.; Cecatiello, V.; Soffientini, P.; Pasqualato, S.; Polo, S. Structure of a ubiquitin-loaded HECT ligase reveals the molecular basis for catalytic priming. *Nat. Struct. Mol. Biol.* **2013**, *20*, 696−701.
(60) Lechtenberg, B. C.; Rajput, A.; Sanishvili, R.; Dobaczewska, M. K.; Ware, C. F.; Mace, P. D.; Riedl, S. J. Structure of a HOIP/E2 ~ ubiquitin complex reveals RBR E3 ligase mechanism and regulation. *Nature* **2016**, *529*, 546−550.
(61) Pickart, C. M. Mechanisms underlying ubiquitination. *Annu. Rev. Biochem.* **2001**, *70*, 503−533.
(62) Faesen, A. C.; Luna-Vargas, M. P.; Geurink, P. P.; Clerici, M.; Merkx, R.; Van Dijk, W. J.; Hameed, D. S.; El Oualid, F.; Ovaa, H.; Sixma, T. K. The differential modulation of USP activity by internal regulatory domains, interactors and eight ubiquitin chain types. *Chem. Biol.* **2011**, *18*, 1550−1561.
(63) Ai, H.; He, Z.; Deng, Z.; Chu, G.-C.; Shi, Q.; Tong, Z.; Li, J.-B.; Pan, M.; Liu, L. Structural and mechanistic basis for nucleosomal H2AK119 deubiquitination by single-subunit deubiquitinase USP16. *Nat. Struct. Mol. Biol.* **2024**, *31*, 1745−1755.
(64) Juang, Y.-C.; Landry, M.-C.; Sanches, M.; Vittal, V.; Leung, C. C.; Ceccarelli, D. F.; Mateo, A.-R. F.; Pruneda, J. N.; Mao, D. Y.; Szilard, R. K.; Orlicky, S.; Munro, M.; Brzovic, P. S.; Klevit, R. E.; Sicheri, F.; Durocher, D. OTUB1 co-opts Lys48-linked ubiquitin recognition to suppress E2 enzyme function. *Mol. Cell* **2012**, *45*, 384−397.

https://doi.org/10.1021/jacsau.5c00067
JACS Au 2025, 5, 2148−2158

(65) Zhang, L.; Deng, Z.; Du, Y.; Xu, Z.; Zhang, T.; Tong, Z.; Ai, H.; Liang, L.-J.; Liu, L. RAD18-catalysed formation of ubiquitination intermediate mimic of proliferating cell nuclear antigen PCNA. *Bioorg. Med. Chem.* **2025**, *117*, 118016.
(66) Han, D.; Cui, Y.; Deng, X.; Li, C.; Zhu, X.; Wang, B.; Chu, G.-C.; Wang, Z. A.; Tang, S.; Zheng, J.-S.; Liang, L.-J.; Liu, L. Mechanically Triggered Protein Desulfurization. *J. Am. Chem. Soc.* **2025**, *147*, 4135−4146.

https://doi.org/10.1021/jacsau.5c00067
JACS Au 2025, 5, 2148−2158